Synthesis of Renewable Diesel Range Alkanes by Hydrodeoxygenation of Palmitic Acid over 5% Ni/CNTs under Mild Conditions

Yanan Duan [1],[†], Ranran Ding [2],[†], Yanchun Shi [1], Xiao Fang [1], Husheng Hu [1], Mingde Yang [1] and Yulong Wu [1],[3],*

[1] Institute of Nuclear and New Energy Technology, Tsinghua University, Beijing 100084, China; dyanan1989@163.com (Y.D.); shiyc18@126.com (Y.S.); fangxiao456@163.com (X.F.); huhusheng123@tom.com (H.H.); yangmd@tsinghua.edu.cn (M.Y.)

[2] School of Chemical Engineering and Technology, Tianjin University, Tianjin 300072, China; ranran0129@126.com

[3] Beijing Key Laboratory of Fine Ceramics, Beijing 100084, China

* Correspondence: wylong@tsinghua.edu.cn; Tel.: +86-10-8979-6086; Fax: +86-10-6977-1464

† Yanan Duan and Ranran Ding contributed equally to this work.

Abstract: Recently, the catalytic upgrading of bio-oil to renewable diesel has been attracting more and more attention. In the current paper, carbon nanotube (CNT)-supported nickel catalysts, namely, 5% Ni/CNTs, were prepared for liquid hydrocarbon production through the deoxygenation of palmitic acid, the model compound of bio-oil under a mild condition of 240 °C reaction temperature and 2 MPa H_2 pressure. The experimental results revealed that the main reaction product was pentadecane (yield of 89.64%) at an optimum palmitic acid conversion of 97.25% via the hydrodecarbonylation (HDC) process. The deoxygenation mechanism for palmitic acid conversion was also investigated. This study provides technical parameters and a theoretical basis for further industrialization in the bio-oil upgrading process.

---

1. Introduction

The worsening pollution induced by the increasing consumption of conventional fossil fuels and the ever-increasing dependency on imported oil make researchers search for eco-friendly energy which is sustainable and renewable [1,2]. Biomass is regarded as the most prospective alternative energy source, as it is the only renewable resource which can be directly translated into liquid carbon fuels, and it is carbon dioxide neutral due to photosynthesis. Generally, bio-oil is the liquid produced from lignocellulosic biomass, such as rice husk, miscanthus, pinewood, cellulose, and lignin, through thermochemical conversion [3,4]; it has some similarities to the chemical composition of petroleum crude and is recognized as the most promising alternative to petroleum, which could improve the nation's energy independence as well as reduce greenhouse gas emissions [5]. However, compared to petroleum, the bio-oil contains a significant quantity of oxygen (up to 35–40 wt %), which results in its lower pH and calorific value, chemical and thermal instability, and poor storage stability [6–9], and these properties make it difficult to directly use bio-oil as the liquid fuel for transportation. So, upgrading of the bio-oil method is needed.

Long-carbon-chain (C_{16}–C_{22}) fatty acids are normally selected as a model compound of bio-oil, especially algae-based bio-oil, to investigate bio-oil upgrading via deoxygenation reactions [10]. After upgrading, long-carbon-chain hydrocarbons are obtained as final products, which can be a

substitution for traditional diesel oil. Recently, there have been three deoxygenation approaches for fatty acids as follows: decarboxylation (DCX: R–COOH → R–H + CO_2), hydrodecarbonylation (HDC: R–COOH + H_2 → R–H + CO + H_2O) and hydrodeoxygenation (HDO: R–COOH + $3H_2$ → R–CH_3 + $2H_2O$) [11–15]; further, three main catalyst systems have been applied to the deoxygenation of fatty acids: (1) NiMo or CoMo sulfide/supported catalysts [16,17]; (2) noble metal–supported catalysts, mainly including Pt- or Pd-based catalysts [1,18–20]; (3) supported non-noble transition metal catalysts (e.g., Fe, Co, Ni, Mo et al.) [21–24]. Sulfide/supported catalysts may contaminate the products as a result of sulfur leaching, and the noble metals are high in price, and these deficiencies restrict the practical usage for the former two catalyst systems. Meanwhile, the supported non-noble transition metal catalysts have the most promising prospect for their high catalytic activity and low cost and are feasible for application in the fatty acid deoxygenation process. In the published literatures, Chao et al. [25] deoxygenated palmitic acid with the presence of water at 300 °C and 0.69 MPa of H_2 pressure over Ni/ZrO_2 and concluded that decarbonylation was the major route to generate 30.2% of C_{15}, 26.0% of C_8–C_{14} and 18.6% of CH_4 as the main products. Imane et al. [26] studied nickel supported on SiO_2 and $γ$-Al_2O_3 performed in HDO of stearic acid in a 3 MPa hydrogen atmosphere at 300 °C, obtaining both 100% acid conversion and 96.3% and 96.2% of n-heptadecane selectivity, respectively. Hui et al. [27] used activated carbon-supported nickel phosphide catalyst in the deoxidation of palmitic acid at 350 °C and 5% H_2/Ar with the rate of 30 mL/min, and found that the coexistence of Ni_2P and $Ni_{12}P_5$ resulted in the optimum C_{15} selectivity of 74.9%. Ning and his colleagues [25,28] examined different metal acetate salts for the catalytic deoxygenation of stearic acid, and found Ni(OAc)$_2$ exhibited the highest activity with 62% yield achieved at 350 °C for 4.5 h with only 1 mol % of the catalyst in the absence of H_2 and solvent; furthermore, they stated the diversified applications of nickel-based bimetallic catalysts for energy and the environment since Ni has a high alloying efficiency with all noble metals as well as many transition metals in different mass ratios.

Our group also explored the hydroconversion of octanoic acid with Ni/ZrO_2 at 320 °C and 3 MPa of H_2, obtaining 69.9% yield of C_7 as the main product through HDC of ocatnoic acid [29]. These papers revealed Ni active particles as promising catalytically active components for fatty acid deoxygenation, but the reaction conditions were too demanding for the reaction temperatures all greater than or equal to 300 °C. It is well known that a relatively higher reaction temperature results in high energy consumption, and can induce undesirable side reactions such as coking or polymerization, which sequentially leads to catalyst deactivation [11]. So, it is meaningful to investigate the deoxygenation of fatty acids under milder conditions. In our other former research, carbon nanotubes (CNTs)-supported MoO_2, Co-MoO_2 or β-Mo_2C catalysts were applied to the conversion of palmitic acid and stearic acid at 220 °C or 180 °C with 4 MPa of H_2, and these catalysts all had sufficient deoxygenation activity to obtain 100% acid conversion with around a 90% yield of alkanes without carbon loss [30–32]. This phenomenon demonstrates that the CNTs are a promising catalyst support since the CNTs have high thermal conductivity, accessibility of the active phase, good chemical stability in aggressive media and a high surface area [33,34]; the unique electronic structure of CNTs exhibits a large charge transfer and deficient electron, as well as gaps, which decrease the diffusion resistance kinetically [35,36]. In addition, the active metal atoms have a stronger interaction with outside CNTs over the supported catalysts, which can also lead to structure defects of CNTs that affect the physical properties and chemical behavior of the catalysts, and further affect the hydrodeoxygenation of the reactant and the transfer of products inside or outside the CNTs [37]. Furthermore, the CNTs possess a hydrophobic surface with relatively few or no functional groups, which decreases the probability of side reactions [38] and promotes water desorption that favors the HDO reaction [39,40]. Although the reaction temperature has been lowered, the high H_2 pressure of 4 MPa is unfavorable to the safety and expense of hydrogenation equipment, so it is of significance to further research fatty acid conversion to alkanes at much milder reaction conditions.

In this paper, CNTs-supported Ni catalyst (5% Ni loading) was synthesized and applied in the deoxygenation of palmitic acid, and the 5% Ni/CNTs catalyst was characterized by XRD (X-ray powder

diffraction), TEM (Transmission electron microscope) and nitrogen sorption. This work aims to design a new style of catalyst, displaying high efficiency for palmitic acid hydroconversion at a milder reaction condition, and hopes to further disclose the deoxygenation mechanism for fatty acids, sequentially contributing to the upgrading of bio-oil.

2. Results and Discussion

2.1. Characterization of Catalyst

The XRD patterns of CNTs and 5% Ni/CNTs are shown in Figure 1. With a hexagonal structure, the diffraction peaks of CNTs distributed at 26.0° and 44.0° [30]. Meanwhile, the diffraction peaks appearing at 2θ of 44.3°, 51.7° and 76.4° are assigned to the planes of (111), (200) and (220) of metal Ni, respectively (JCPDS: 65-0380). Only Ni^0 and CNTs were observed by XRD. It can be verified that Ni/CNTs catalyst was formed in sample (b), and the Ni^0 was dispersed in the CNT support. Additionally, well-crystallized structures were indicated in samples (a) and (b) with narrow and intensive diffraction peaks.
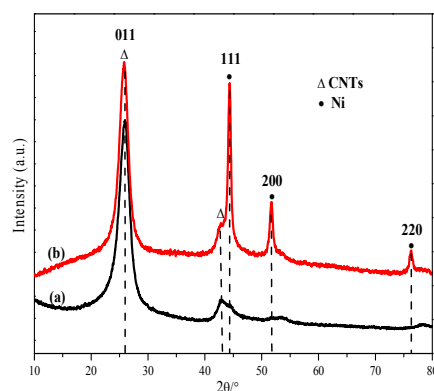

Figure 1. XRD patters for CNTs (a) and 5% Ni/CNTs (b).

The typical N_2 adsorption-desorption isotherm and BJH (Barrett-Joyner-Halenda) pore size distribution plot of 5% Ni/CNTs are displayed in Figure 2. A representative-type IV curve was exhibited in the nitrogen adsorption-desorption isotherm with sharp capillary condensation steps at relative pressures of 0.8–0.98 (Figure 2a) [41]. The H1-type hysteresis loop demonstrates the typical mesoporous material property [42]. In addition, from Figure 2b, the narrow pore size distribution of 5% Ni/CNTs was 2.7 nm.
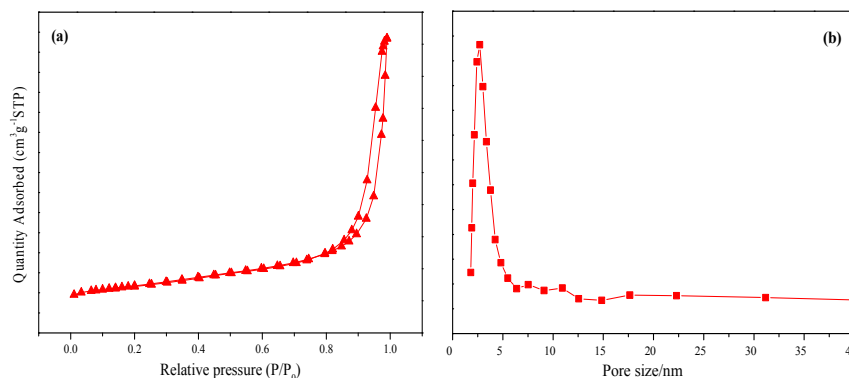

Figure 2. N_2 sorption-desorption isotherm (**a**) and pore size distribution (**b**) of 5% Ni/CNTs.

To further study the particle distribution, shape and size of 5% Ni/CNTs, TEM images of 5% Ni/CNTs are shown in Figure 3. A relatively uniform distribution of nanoparticles was displayed on the CNTs' surface. Figure 3a shows that spherical nanostructured Ni particles were well distributed on the surface of CNTs with an average Ni particle size of 10 nm with no evident agglomerations observed. It is considered that the CNTs-supported Ni catalyst reveals a model of "support dispersion", for CNTs can disperse Ni particles adequately and take on sintering barriers efficiently to restrain Ni particles from sintering. The high-resolution TEM (HRTEM) image of 5% Ni/CNTs is shown in Figure 3b, and a lattice distance of 0.20 nm was obtained, which can be assigned to the (111) plane of the metal Ni phase [43]. This indicates that the synthetic method is facile for CNTs to be uploaded individual Ni nanoparticles.
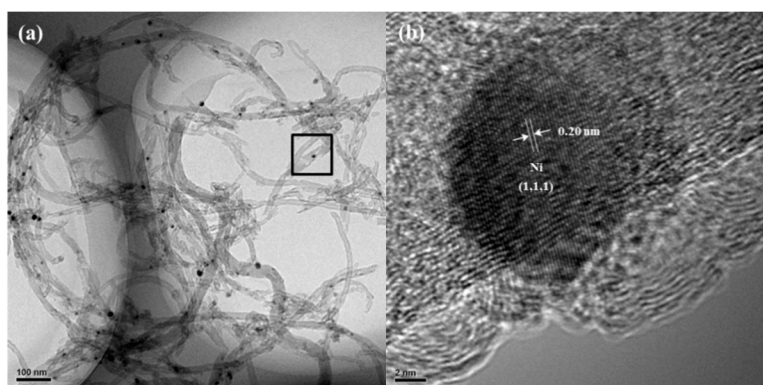

Figure 3. TEM (Transmission electron microscope) images of 5% Ni/CNTs.

2.2. Deoxygenation at Different Temperatures

As a significant parameter, temperature affects both the reaction rate and equilibrium. The conversion of palmitic acid and detailed distributions of the products over 5% Ni/CNTs with the changes in temperature are summarized in Figure 4. The palmitic acid conversion increased distinctly when the reaction temperature was below 240 °C, at which a conversion of 97.25% was obtained. Continuously increasing the reaction temperature to 260 °C, the palmitic acid conversion rose to 100% slowly, and no more conversions were obtained. From Figure 4, the main product of palmitic acid deoxygenation was pentadecane with one carbon loss through decarbonylation, and the yield was changed significantly with the rise of the temperature. With the temperature increasing, the conversion rose to 240 °C, at which the highest yield of 89.64% for pentadecane was achieved. Further increasing the temperature to 280 °C, the yield of pentadecane decreased to 38.43% dramatically, meanwhile the yield of light alkanes generated through cracking increased from 5.34% to 59.64% when the temperature increased from 240 °C to 280 °C. This shows that a temperature higher than 240 °C favors hydrocracking at the cost of decarbonylation. Hence, the desired temperature is 240 °C. A larger amount of hexadecanol with a yield of 4.63% produced by palmitic acid hydrogenation was observed at a lower temperature of 220 °C; further increasing the reaction temperature to 240 °C, the hexadecanol almost disappeared through the dehydration process to generate hexadecane, which suggests a higher temperature barrier for the dehydration of alcohol. Due to the small amount of hexadecene and the very reactive C=C bond, there was no hexadecene detected in the reaction process. Besides, through the deoxgenation process, a certain amount of hexadecane was also observed, which was produced through a sequence of hexadecanol dehydration-hydrogenation reactions; further, the yield of hexadecane was 2.47% at a reaction temperature of 240 °C.
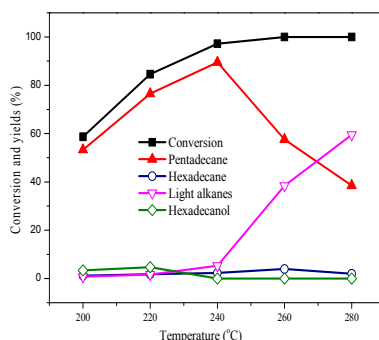
Figure 4. The product distributions of palmitic acid conversion at different temperatures over 5% Ni/CNTs. Reaction conditions: palmitic acid (0.5 g), decane (50 mL), catalyst (0.25 g), H_2 2 MPa, reaction time 4 h.

2.3. Deoxygenation at Different Hydrogen Pressures

The initial hydrogen pressure is a prominent parameter that affects the deoxygenation rate of palmitic acid. Figure 5 showed the palmitic acid conversion and product distributions over 5% Ni/CNTs as the function of H_2 partial pressure. The yield of pentadecane and the conversion of palmitic acid were proportional to the hydrogen pressure until the pressure was increased to 2 MPa, at which the optimum values of 97.25% acid conversion and 89.64% pentadecane yield were achieved, respectively. Further elevating the hydrogen pressure, the palmitic acid conversion and pentadecane selectivity started to decrease distinctly, for a specified volume of H_2 can restrain the carbon deposition on a catalyst's surface which is beneficial for the activity; nevertheless, too much hydrogen would contend for the adsorption sites with palmitic acid [29], so a decreased tendency appeared when the hydrogen pressure exceeded 2 MPa.
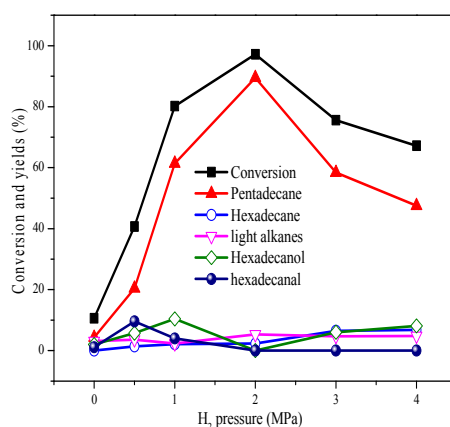

Figure 5. The product distributions of catalytic hydrogenation of palmitic acid under different hydrogen pressures over 5% Ni/CNTs. Reaction conditions: palmitic acid (0.5 g), decane (50 mL), catalyst (0.25 g), reaction temperature 240 °C, reaction time 4 h.

From Figure 5, it can also be concluded that the yield of hexadecane increased with the increase of the hydrogen pressure, and reached 6.75% when the hydrogen pressure was 4 MPa. Meanwhile, the yields of hexadecanal and hexadecanol reached maximum values of 9.85% and 10.32% at lower hydrogen pressures of 0.5 MPa and 1 MPa, respectively Equilibrium exists between hexadecanal and hexadecanol, and hydrogen is necessary to convert hexadecanal into hexadecanol. These results were in accordance with the preceding reports that low hydrogen pressure raised the selectivity of decarbonylation to generate pentadecane, whereas high hydrogen pressures benefited

the HDO of palmitic acid to produce hexadecane [44]. A certain amount of light alkanes also existed, which accounted for about 5% and had little change with the increase of the hydrogen pressures.

2.4. Deoxygenation Mechanism on 5% Ni/CNTs

To research the catalytic performance of 5% Ni/CNTs for palmitic acid conversion as a function of time, we took and detected the liquid products every 30 min during the reaction process, and the results are shown in Figure 6. The final conversion of palmitic acid was 97.25% with the yield of 89.64% for pentadecane, 2.47% for hexadecane, 5.34% for light alkanes, 0.31% for hexadecanal and hexadecanol over 5% Ni/CNTs at 240 °C in an atmosphere of 2 MPa H_2. Hexadecanal was the initial product and it reached a maximum yield of 9.85% at 60 min, and then decreased rapidly to 0.31% at 240 min. Meanwhile, the yield of hexadecanol increased gradually and reached the maximum of 13.89% after 90 min, which then decreased to 0.31% eventually. Hexadecanal was in equilibrium with hexadecanol. The major product pentadecane, produced through hexadecanal decarbonylation, increased gradually with the reaction progressing. Hydrocarbons with fewer than 15 carbon atoms were produced through cracking over acid sites or hydrogenolysis over metallic sites of 5% Ni/CNTs [45]. The yield of light hydrocarbons increased continuously, and increased to 5.34% eventually. Resulting from hexadecanol dehydration-hydrogenation reactions, a small quantity of hexadecane was also detected in the product. Because of the fast hydrogenation rate and low yield of the double bond, the hexadecanol dehydration product hexadecene was not detected.
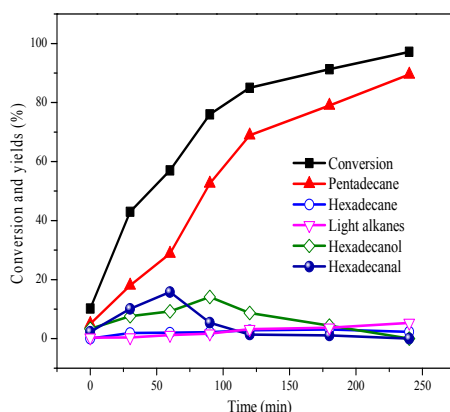

Figure 6. The product distributions of catalytic hydrogenation of palmitic acid at different reaction times over 5% Ni/CNTs. Reaction conditions: palmitic acid (0.5 g), decane (50 mL), catalyst (0.25 g), reaction temperature 240 °C, hydrogen pressure 2 MPa.

Table 1 summarizes the experimental results of the deoxygenation of different fatty acids over nickel- or molybdenum-based catalysts that our group has published before. From [29], 0.5 g of 5% Ni/ZrO$_2$ catalyst was applied to the deoxygenation of octanoic acid (1 g) with 100 mL solvent in a 150 mL stainless autoclave, obtaining 92.79% acid conversion at a high reaction temperature of 320 °C and a H_2 pressure of 3 MPa with the main product of heptane (yield of 69.68%) which was generated through octanoic acid HDC. When a Mo particle was introduced into 5% Ni/ZrO$_2$ to generate 10% Mo–5% Ni/ZrO$_2$, the main product for octanoic acid deoxygenation was octane with a yield of 77.07% through the HDO process. In our other work [30], the removal of oxygen from the long-chain fatty acid palmitic acid was studied with 0.25 g of 5% MoO$_2$/CNTs as a catalyst at a relatively low reaction temperature of 220 °C and a higher H_2 pressure of 4 MPa in a 150 mL autoclave with 50 mL solvent, obtaining a 92.20% yield of hexadecane as the main product. In our previous work [31], we further modified 5% MoO$_2$/CNTs by doping 1.5% Co particles, and applied it into the deoxygenation process of palmitic acid, achieving a 89.30% yield of hexadecane at a lower reaction temperature of 180 °C. Our group also put the CNTs-supported molybdenum catalyst into use for the

deoxygenation of stearic acid, revealing that HDO was prevailing and octadecane was the leading product with a yield of 91.24% in the deoxygenation process [32]. These catalysts all had outstanding catalytic activity for fatty acid conversions; however, the reaction systems consumed too much H_2 (4 MPa) which increased the cost of the hydrogenation equipment. In this paper, we investigated palmitic acid deoxygenation using 5% Ni/CNTs as catalyst at a mild condition of a 240 °C reaction temperature with only 2 MPa H_2 pressure, and obtained 97.25% palmitic acid conversion, 89.64% pentadecane yield through HDC and 2.47% hexadecane yield via HDO. Besides, we also proposed a reasonable reaction pathway for fatty acid conversion over the 5% Ni/CNTs catalyst in Scheme 1.

Table 1. Experimental results for fatty acid deoxygenation that our group has published.

Reactant	Catalyst	$V_{reactor}$ (mL)	$V_{solvent}$ (mL)	W_{acid} (g)	$W_{catalyst}$ (g)	T (°C)	P_{H2} (Mpa)	Con. (%)	Main product Distribution (%)		Ref.
Octanoic acid	5% Ni/ZrO$_2$	250	100	1	0.5	320	3	92.79	Heptane/69.68	Octane/5.00	[29]
Octanoic acid	10% Mo-5% Ni/ZrO$_2$	250	100	1	0.5	320	3	100	Heptane/10.67	Octane/77.07	[29]
Palmitic acid	5% MoO$_2$/CNTs	150	50	0.5	0.25	220	4	100	Pentadecan/7.60	Hexadecane/92.20	[30]
Palmitic acid	1.5% Co-5% MoO$_2$/CNTs	150	50	0.5	0.1	180	4	100	Pentadecan/5.20	Hexadecane/89.30	[31]
Stearic acid	β-Mo$_2$C/CNTs	150	50	0.5	0.25	180	4	100	Heptadecan/8.76	Octadecan/91.24	[32]
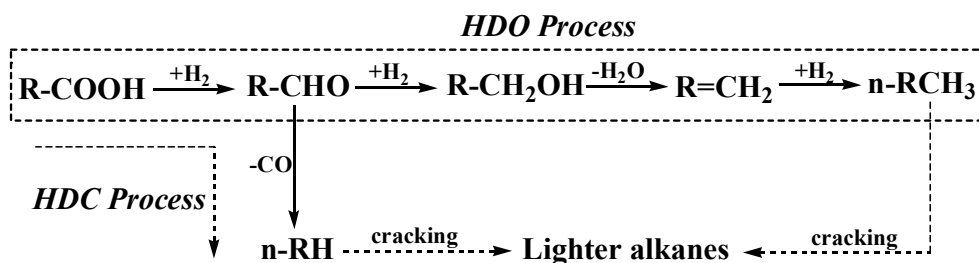
Scheme 1. Proposed reaction pathway of fatty acid conversion on 5% Ni/CNTs.

Combined with the results of palmitic acid conversion in this paper, Scheme 1 showed the fatty acid deoxygenation mechanism over the 5% Ni/CNTs catalyst. Firstly, the fatty acids hydrogenated to aldehydes over the nickel active sites, and most generated aldehydes preferred to convert into hydrocarbons with one-carbon loss via the HDC process for palmitic acid to produce 89.64% of pentadecane as the main product. Meanwhile, a small amount of aldehydes hydrogenated to alcohols, and then through successive dehydration and hydrogenation, they generated alkanes without carbon loss via the HDO routine as the minor reaction pathway. A small quantity of lighter alkanes was also generated, which was produced by hydrogenolysis over metallic sites or by cracking over acid sites. The experimental results mentioned above also revealed that the different kinds of active components might impact the deoxygenation pathways for fatty acids, which deserves to be further investigated in detail.

3. Experimental

3.1. Catalysts Preparation

Ni/CNTs catalyst (5% Ni loading) was synthesized by incipient- wetness impregnation method: CNT support was impregnated in a desired concentration of aqueous Ni(NO$_3$)$_2$·6H$_2$O solution, and the metal ion was incorporated into CNTs at room temperature for over 4 h. After drying for 12 h at 105 °C, the catalyst was calcined for 3 h in air and reduced for 4 h in hydrogen at 500 °C with the rate of 80 mL·min^{-1}. All the chemicals were purchased from Shanghai Macklin Biochemical Coltd, Shanghai, China.

3.2. Catalysts Characterization

A Micromeritics ASAP2010 instrument was used to measure N_2-adsorption isotherm at -196 °C. Typically, the sample was degassed for 3 h at 300 °C firstly. The surface area was calculated through Brunauer–Emmett–Teller (BET) method. A FEI tecnai F20 instrument was applied to Transmission electron microscope (TEM, FEI F20 Field Emission Electron Microscope). The Powder X-ray diffraction (PXRD) patterns were recorded on a Bruker D8 Advance X-ray diffractometer (D/MAX-2500) with the Cu K_α radiation (36 kV, 20 mA, λ: 0.1541 nm, scanning step: 2°·min^{-1}). Data were recorded in the 2θ range of 5°–80°.

3.3. Activity Measurements

A 150 mL stainless autoclave was selected to study the catalytic reaction. The autoclave was heated by the electrical furnace and the temperature was tested by a thermocouple, which was controlled to $\pm$ 1 °C. Typically, 0.5 g palmitic acid as reactant and 0.25 g catalyst were placed in the reactor with 50 mL of decane as the solvent. The reactor was purged with H_2 for three times and then pressurized to 2 MPa at room temperature. Next, the sealed reactor was heated at 240 °C for 240 min with the stir rate of 300 rpm. After the reactor being cooled down, 1 µL products was injected in the Agilent GC6820 with a FID (hydrogen flame ionization detector, Agilent, Santa Clara, CA, USA) detector and the GsBP-Inowax capillary column (30 m × 0.32 mm × 0.25 µm). The detect and the inlet temperatures were 280 °C, and split ratio was 10:1. The column temperature starting at 50 °C for 2 min, was increased to 220 °C by the rate of 10 °C·min^{-1} and holding for 5 min.

Conversion = (moles of the converted reactant / moles of the gross reactant) × 100%;

Yield = (moles of each product / moles of total product) × 100%

4. Conclusions

The 5% Ni/CNTs catalysts was synthesized and applied in the deoxygenation of palmitic acid under relatively mild conditions of a 240 °C reaction temperature and 2 MPa H_2 pressure, obtaining 97.25% of palmitic acid conversion with a yield of 69.68% for pentadecane as the main product. The catalyst was characterized through XRD, TEM and nitrogen sorption methods, and the results showed a relatively symmetrical distribution of Ni nanoparticles on the surface of CNTs with a mesoporous material property. In addition, this paper summarized the fatty acid deoxygenation results, and proposed that HDC process was the major reaction routine for fatty acid deoxygenation over 5% Ni/CNTs.

Author Contributions: Yulong Wu and Mingde Yang conceived and designed the experiments; Yanan Duan and Ranran Ding performed the experiments; Yanchun Shi and Xiao Fang analyzed the data; Husheng Hu contributed reagents/materials/analysis tools; Yanan Duan and Ranran Ding wrote the paper.

Conflicts of Interest: The authors declare no conflict of interest.

References

1.　Payormhorm, J.; Kangvansaichol, K.; Reubroycharoen, P.; Kuchonthara, P.; Hinchiranan, N. Pt/Al_2O_3-catalytic deoxygenation for upgrading of Leucaenaleucocephala-pyrolysis oil. *Bioresour. Technol.* **2013**, *139*, 128–135. [CrossRef] [PubMed]

2.　Zhao, C.; Bruck, T.; Lercher, J.A. Catalytic deoxygenation of microalgae oil to green hydrocarbons. *Green Chem.* **2013**, *15*, 1720–1739. [CrossRef]

3.　Lee, E.H.; Park, R.S.; Kim, H.; Park, S.H.; Jung, S.C.; Jeon, J.K.; Kim, S.C.; Park, Y.K. Hydrodeoxygenation of guaiacol over Pt loaded zeolitic materials. *J. Ind. Eng. Chem.* **2016**, *37*, 18–21. [CrossRef]

4. Lee, H.; Kim, Y.M.; Lee, I.G.; Jeon, J.K.; Jung, S.C.; Chung, J.D.; Choi, W.G.; Park, Y.K. Recent advances in the catalytic hydrodeoxygenation of bio-oil. *Korean J. Chem. Eng.* **2016**, *33*, 3299–3315. [CrossRef]

5. Tang, Y.; Yu, W.J.; Mo, L.Y.; Lou, H.; Zheng, X.M. One-Step Hydrogenation-Esterification of Aldehyde and Acid to Ester over Bifunctional Pt Catalysts: A Model Reaction as Novel Route for Catalytic Upgrading of Fast Pyrolysis Bio-Oil. *Energy Fuels* **2008**, *22*, 3484–3488. [CrossRef]

6. Roh, H.S.; Eum, I.H.; Jeong, D.W.; Yi, B.E.; Na, J.G.; Ko, C.H. The effect of calcination temperature on the performance of Ni/MgO-Al_2O_3 catalysts for decarboxylation of oleic acid. *Catal. Today* **2011**, *164*, 457–460. [CrossRef]

7. Ma, B.; Hu, J.B.; Wang, Y.M.; Zhao, C. Ni nanoparticles encapsulated into mesoporous single-crystalline HBEA: Application for drainage oil hydrodeoxygenation to diesel. *Green Chem.* **2015**, *17*, 4610–4617. [CrossRef]

8. Chen, Y.; Wu, Y.L.; Ding, R.R.; Zhang, P.; Liu, J.; Yang, M.D. Catalytic hydrothermal liquefaction of D. tertiolecta for the production of bio-oil over different acid/base catalysts. *AIChE J.* **2015**, *61*, 1118–1128. [CrossRef]

9. Duan, P.G.; Savage, P.E. Catalytic hydrotreatment of crude algal bio-oil in supercritical water. *Appl. Catal. B Enviorn.* **2011**, *104*, 136–143. [CrossRef]

10. Peng, B.X.; Zhao, C.; Kasakov, S.; Foraita, S.; Lercher, J.A. Manipulating Catalytic Pathways: Deoxygenation of Palmitic Acid on Multifunctional Catalysts. *Chem. Eur. J.* **2013**, *19*, 4732–4741. [CrossRef] [PubMed]

11. Jimenez, E.S.; Crocker, M. Catalytic deoxygenation of fatty acids and their derivatives to hydrocarbon fuels via decarboxylation/decarbonylation. *J. Chem. Technol. Biotechnol.* **2012**, *87*, 1041–1050. [CrossRef]

12. Zhang, S.P.; Yan, Y.J.; Ren, Z.W.; Li, T.C. Study of hydrodeoxygenation of bio-oil from the fast pyrolysis of biomass. *Energy Sources* **2003**, *25*, 57–65.

13. Mortensen, P.M.; Grunwaldt, J.D.; Jensen, P.A.; Knudsen, K.G.; Jensen, A.D. A review of catalytic upgrading of bio-oil to engine fuels. *Appl. Catal. A Gen.* **2011**, *407*, 1–19. [CrossRef]

14. Guan, J.; Peng, G.M.; Cao, Q.; Mu, X.D. Role of MoO_3 on a Rhodium catalyst in the selective hydrogenolysis of biomass-derived tetrahydrofurfuryl alcohol into 1,5-pentanediol. *J. Phys. Chem. C* **2014**, *118*, 25555–25566. [CrossRef]

15. Zhang, X.H.; Wang, T.J.; Ma, L.L.; Zhang, Q.; Jiang, T. Hydrotreatment of bio-oil over Ni-based catalyst. *Bioresour. Technol.* **2013**, *127*, 306–311. [CrossRef] [PubMed]

16. Donnis, B.; Egeberg, R.G.; Blom, P.; Knudsen, K.G. Hydroprocessing of bio-oils and oxygenates to hydrocarbons. Understanding the reaction routes. *Top. Catal.* **2009**, *52*, 229–240. [CrossRef]

17. Liu, Y.; Sotelo, B.R.; Murata, K.; Minowa, T.; Sakanishi, K. Hydrotreatment of jatropha oil to produce green diesel over trifunctional Ni–Mo/SiO_2–Al_2O_3 catalyst. *Chem. Lett.* **2009**, *38*, 552–553. [CrossRef]

18. Immer, J.G.; Kelly, M.J.; Lamb, H.H. Catalytic reaction pathways in liquid-phase deoxygenation of C_{18} free fatty acids. *Appl. Catal. A* **2010**, *375*, 134–139. [CrossRef]

19. Matthias, A.; Thomas, N.; Wolfgang, F.H.; Jürgen, F.; Jeremie, G. Catalytic deoxygenation of oleic acid in continuous gas flow for the production of diesel-like hydrocarbons. *Appl. Catal. A Gen.* **2011**, *399*, 198–204.

20. Kubiclied, I.; Snare, M.; Eranen, K.; Maki, A.P.; Murzin, D.Y. Hydrocarbons for diesel fuel via decarboxylation of vegetable oils. Catal. *Today* **2005**, *106*, 197–200.

21. Kandel, K.; Anderegg, J.W.; Nelson, N.C.; Chaudhary, U.; Slowing, I.I. Supported iron nanoparticles for the hydrodeoxygenation of microalgal oil to green diesel. *J. Catal.* **2014**, *314*, 142–148. [CrossRef]

22. Gusmao, J.; Brodzki, D.; Djega, M.G.; Frety, R. Utilization of vegetable oils as an alternative source for diesel-type fuel: Hydrocracking on reduced Ni/SiO_2 and sulphided Ni-Mo/C-Al_2O_3. *Catal. Today* **1989**, *5*, 533–544. [CrossRef]

23. Li, W.J.; Gao, Y.J.; Yao, S.Y.; Ma, D.; Yan, N. Effective deoxygenation of fatty acids over Ni(OAc)$_2$ in the absence of H_2 and solvent. *Green Chem.* **2015**, *17*, 4198–4205. [CrossRef]

24. Han, J.X.; Duan, J.D.; Chen, P.; Lou, H.; Zheng, X.M.; Hong, H.P. Carbon-supported molybdenum carbide catalysts for the conversion of vegetable oils. *ChemSusChem* **2012**, *5*, 727–733. [CrossRef] [PubMed]

25. Miao, C.; Flores, O.M.; Davidson, S.D.; Li, T.T.; Dong, T.; Gao, D.F.; Wang, Y.; Garcia, P.M.; Chen, S.L. Hydrothermal catalytic deoxygenation of palmitic acid over nickel catalyst. *Fuel* **2016**, *166*, 302–308. [CrossRef]

26. Hachemi, I.; Jeništová, K.; Arvela, P.M.; Kumar, N.; Eränen, K.; Hemming, J.; Murzin, D.Y. Comparative study of sulfur-free nickel and palladium catalysts in hydrodeoxygenation of different fatty acid feedstocks for production of biofuels. *Catal. Sci. Technol.* **2016**, *6*, 1476–1487. [CrossRef]

27. Xin, H.; Guo, K.; Li, D.; Yang, H.Q.; Hu, C.W. Production of high-grade diesel from palmitic acid over activated carbon-supported nickel phosphide catalysts. *Appl. Catal. B Enviorn.* **2016**, *187*, 375–385. [CrossRef]

28. De, S.; Jiaguang, J.G.; Luque, R.; Yan, N. Ni-based bimetallic heterogeneous catalysts for energy and environmental applications. *Energy Environ. Sci.* **2016**, *9*, 3314–3347. [CrossRef]

29. Duan, Y.N.; Wu, Y.L.; Zhang, Q.H.; Ding, R.R.; Chen, Y.; Liu, J.; Yang, M.D. Towards conversion of octanoic acid to liquid hydrocarbon via hydrodeoxygenation over Mo promoter nickel-based catalyst. *J. Mol. Catal. A Chem.* **2015**, *398*, 72–78. [CrossRef]

30. Ding, R.R.; Wu, Y.L.; Chen, Y.; Liang, J.M.; Liu, J.; Yang, M.D. Effective hydrodeoxygenation of palmitic acid to diesel-like hydrocarbons over MoO_2/CNTs catalyst. *Chem. Eng. Sci.* **2015**, *135*, 517–525. [CrossRef]

31. Ding, R.R.; Wu, Y.L.; Chen, Y.; Chen, H.; Wang, J.L.; Shi, Y.C.; Yang, M.D. Catalytic hydrodeoxygenation of palmitic acid over a bifunctional Co-doped MoO_2/CNTs catalyst: An insight into the promoting effect of cobalt. *Catal. Sci. Technol.* **2016**, *6*, 2065–2076. [CrossRef]

32. Liang, J.M.; Ding, R.R.; Wu, Y.L.; Chen, Y.; Wu, K.J.; Meng, Y.Q.; Yang, M.D.; Wang, Y.W. Effective conversion of heteroatomic model compounds in microalgae-based bio-oils to hydrocarbons over β-Mo_2C/CNTs catalyst. *J. Mol. Catal. A Chem.* **2016**, *411*, 95–102. [CrossRef]

33. Li, C.; Shao, Z.F.; Pang, M.; Williams, T.C.; Zhang, X.F.; Liang, C.H. Carbon nanotubes supported mono-and bimetallic Pt and Ru catalysts for selective hydrogenation of phenylacetylene. *Ind. Eng. Chem. Res.* **2012**, *51*, 4934–4941. [CrossRef]

34. Dongil, A.B.; Bachiller, B.B.; Rodriguez, I.R.; Fierro, J.L.G.; Escalona, N. The effect of Cu loading on Ni/carbon nanotubes catalysts for hydrodeoxygenation of guaiacol. *RSC Adv.* **2016**, *6*, 26658–26667. [CrossRef]

35. Chen, W.; Pan, X.; Bao, X. Tuning of redox properties of iron and iron oxides via encapsulation within carbon nanotubes. *JASC* **2007**, *129*, 7421–7426. [CrossRef] [PubMed]

36. Chen, W.; Fan, Z.; Pan, X.; Bao, X.H. Effect of confinement in carbon nanotubes on the activity of Fischer—Tropsch iron catalyst. *JASC* **2008**, *130*, 9414–9419. [CrossRef] [PubMed]

37. Charlier, J.C. Defects in carbon nanotubes Accounts. *Chem. Res.* **2002**, *35*, 1063–1069. [CrossRef]

38. Prasomsr, T.; Shetty, M.; Murugappan, K.; Leshkov, Y.R. Insights into the catalytic activity and surface modification of MoO_3 during the hydrodeoxygenation of lignin-derived model compounds into aromatic hydrocarbons under low hydrogen pressures. *Energy Environ. Sci.* **2014**, *7*, 2660–2669. [CrossRef]

39. Yang, H.; Song, S.; Rao, R.; Wang, X.Z.; Yu, Q.; Zhang, A.M. Enhanced catalytic activity of benzene hydrogenation over nickel confined in carbon nanotubes. *J. Mol. Catal. A Chem.* **2010**, *323*, 33–39. [CrossRef]

40. Serp, P.; Castillejos, E. Catalysis in carbon nanotubes. *ChemCatChem* **2010**, *2*, 41–47. [CrossRef]

41. Selvaraj, M.; Shanthi, K.; Maheswari, R.; Ramanathan, A. Hydrodeoxygenation of guaiacol over MoO_3-NiO/ mesoporous silicates: Effect of incorporated heteroatom. *Energy Fuels* **2014**, *28*, 2598–2607. [CrossRef]

42. Biabani, R.A.; Rezaei, M.; Fattah, Z. Low-temperature CO oxidation over nanosized Fe-Co mixed oxide catalysts: Effect of calcination temperature and operational conditions. *Chem. Eng. Sci.* **2013**, *94*, 237–244. [CrossRef]

43. Li, F.J.; Zhang, S.; Lee, J.W.; Guo, J.; White, T.J.; Li, B.; Zhao, D.L. Orientation of silicon nanowires grown from nickel-coated silicon wafers. *J. Cryst. Growth* **2014**, *404*, 26–33. [CrossRef]

44. Boda, L.; Onyestyák, G.; Solt, H.; Lónyi, F.; Valyon, J.; Thernesz, A. Catalytic hydroconversion of tricaprylin and caprylic acid as model reaction for biofuel production from triglycerides. *Appl. Catal. A Gen.* **2010**, *374*, 158–169. [CrossRef]

45. Peng, B.X.; Yao, Y.; Zhao, C.; Lercher, J.A. Towards quantitative conversion of microalgae oil to diesel-range alkanes with bifunctional catalysts. *Angew. Chem. Int. Ed.* **2012**, *124*, 2114–2117. [CrossRef]